New Application of Evanescent Mode Waveguide to Filter Design

RICHARD V. SNYDER, MEMBER, IEEE

Abstract—**Evanescent waveguide (rectangular or round) sections are used in conjunction with an admittance inverter synthesis technique incorporating frequency variable turns ratios to realize wide-band microwave (up to 1 octave) and low-frequency (60-MHz) low-loss bandpass filters. This work extends and corrects previous published information.**

I. Introduction

In an informative paper, Craven and Mok [1] applied network synthesis techniques to lengths of below cutoff waveguide to obtain evanescent bandpass filters. It is the purpose of this paper to extend their work, introduce some slight corrections, and present various examples of the technique, including extension to low-frequencies (down to 60 MHz) and to broad-band filters (up to an octave). For wide stopband applications (no spurious recoveries until at least $1.5f_0$) the structures will be shown to be more volumetrically efficient than others available.

II. Historical Difficulties

The work in [1], [8], and [9], has several limitations which must be overcome for general utilization of the technique. Filters designed using the methods contained in these references require that coupling reactances be invariant. This requirement limits the bandwidth over which an insertion loss function can be accurately predicted to 20 percent or less. Parasitic characteristics of the resonator capacitors were not included; thus bandwidth shrinkage and increased passband ripple resulted. Certain errors in the discontinuity susceptance formulas made difficult the realization of filters terminating in propagating waveguide. Data were not available on the Q of nonrectangular cross sections. It was difficult to compute the length of the resonator capacitors. Finally, coupling methods presented were not suitable for broad bandwidths.

III. Design Technique and Results

The synthesis approach of [1] is illustrated in [1, Fig. 3]. The admittance inverters utilize a simple equivalent circuit an inductive PI section. Our approach is patterned after Levy [2]. A more complete admittance inverter model is used in Fig. 1 which incorporates transformers with frequency variable turns ratio. An equivalence similar to [2, Fig. 8] is developed, with hyperbolic functions replacing circular functions. The use of a frequency variable turns ratio enables extension of the design technique of [1] to a full octave bandwidth. The synthesis is indicated in Fig. 3, with all relevant equations summarized, for the shunt resonator case.

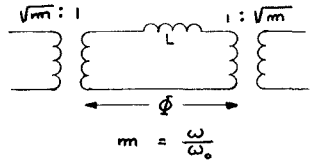

Fig. 1. Admittance inverter equivalent circuit.

These equations enable the relation of the prototype transformer bandwidth to the filter length distribution resulting in a filter with the specified passband. Craven and Mok [1] have derived a correction factor between the frequency dependencies of the evanescent guide elements and those of the equivalent lumped elements. Applying this factor Δ and then equating the resultant network to the lumped equivalent network results in the design equations summarized in Fig. 3. Using (2g) and (2h), it is possible to utilize existing transformer tables by adjusting the distributed prototype bandwidth. Our approach thus combines "lumped element" and "distributed element" approaches, where the element values are obtained from existing prototype tables (or are approximated) but are adjusted to compensate both for the lack of harmonic response and for the not-quite-lumped element nature of the structure. For example, using $\theta'_0 = 36°$ [2, example 3], $W''_q = 0.799$, $W = 0.4$, $\phi'_0 = 14.3°$, $W'_q = 0.996$, and the tabulated W_q to be used is 0.64 [from (2h)].

For filters with large bandwidths, it is necessary to work far enough below cutoff that (2) of Fig. 3 has little variation due to change in Δ. For $f_c/f_0 = 8$, an octave filter designed with a ripple of 0.01 dB achieved an actual ripple of approximately 0.1 dB (1.36 VSWR). The response is shown in Fig. 7. Fig. 2 illustrates the reactance versus frequency characteristics of the equivalent elements comprising various lengths of below cutoff square waveguide. The dependencies far below cutoff are almost identically those of lumped inductors.

The actual design is accomplished through the use of an iterative computer program which apportions the inductive equivalent elements of the resonating capacitor to the series and shunt equivalent evanescent elements and thus "moves" the initially computed center spacing of the elements to compensate for their nonzero inductance. This inductance, uncompensated, effectively increased the series coupling

Manuscript received May 2, 1977; revised July 18, 1977.

The author is with Frequency Engineering Laboratories, Farmingdale, NJ 07727.

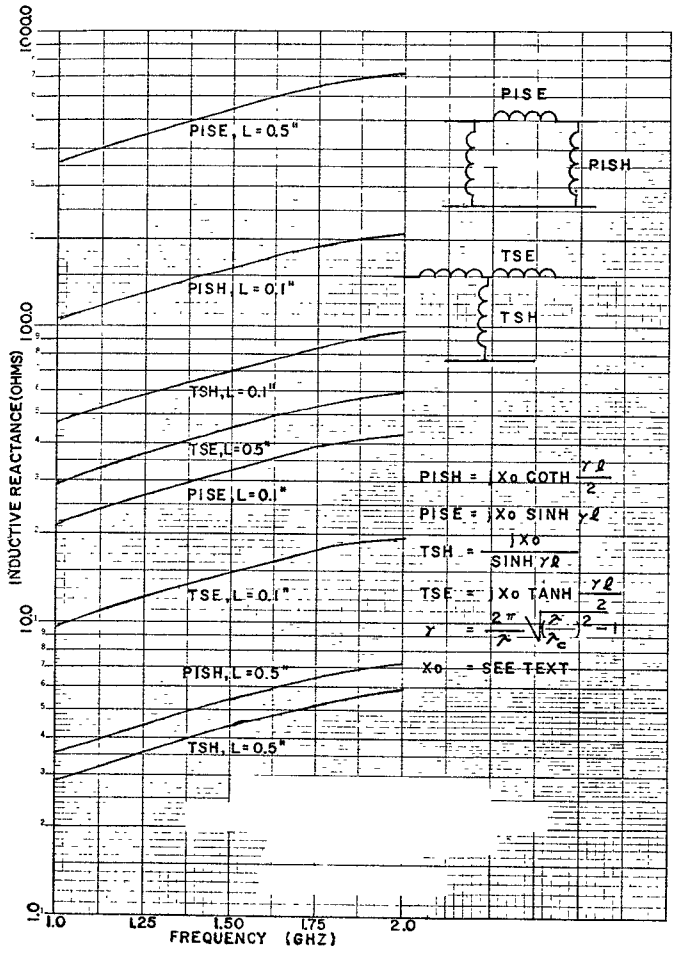

(a)

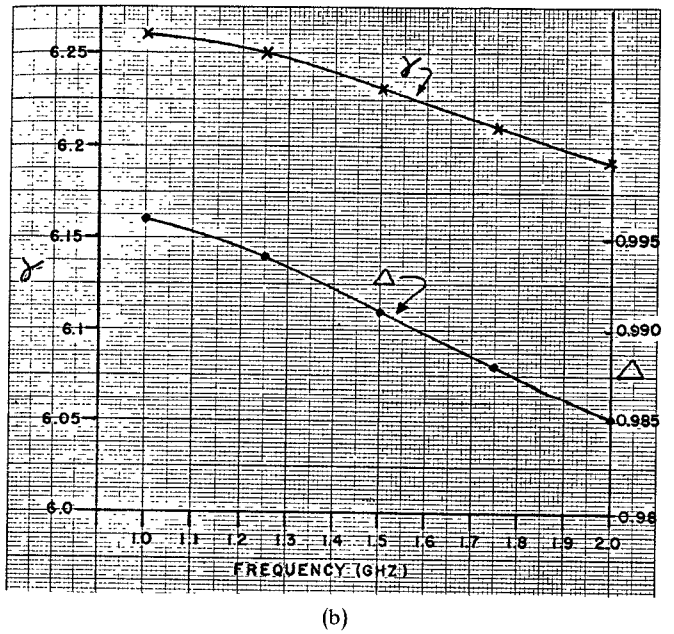

(b)

Fig. 2. (a) Reactance versus frequency. Equivalent circuit elements for two lengths of evanescent guide (0.5 by 0.5 in). (b) γ and Δ versus frequency (0.5 by 0.5 in cross section).

reactance, thus decreasing the filter bandwidth. A procedure similar to that of Fig. 3 can be derived for filters starting with series resonators. The equivalent circuit is similar to [1, Fig. 5], modified per (2) of our Fig. 3. Filters of this type, as in [1], are suitable for termination by above cutoff waveguide. Such a junction results in a combination E-plane, H-plane discontinuity. Using the method of Lewin [3], [(31) and (32) of 1]

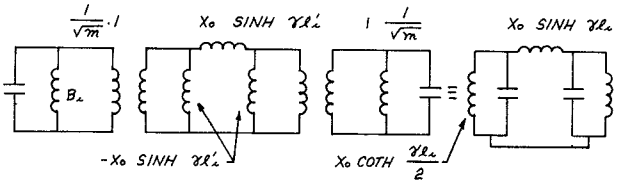

(1a) $B_\lambda = B_0 (\coth \gamma l'_{\lambda-1} + \coth \gamma l'_\lambda)$

(1b) $B_\lambda = \frac{B_0}{m} (\coth \gamma l_{\lambda-1} + \coth \gamma l_\lambda)$

WHERE

(2a) $\sinh \gamma l'_\lambda = \frac{\sqrt{V_{\lambda,\lambda-1}} - \sqrt{V_{\lambda,\lambda+1}}}{\left(\frac{W_g}{W}\right)(\Delta)}$ (SEE EQ 6 & NOTES)

AND

l'_λ = CENTER-TO-CENTER SPACING BETWEEN λ^{TH} AND $(\lambda+1)^{TH}$ CAPACITOR

B_λ = SUSCEPTANCE OF λ^{TH} SHUNT INDUCTANCE (OR λ^{TH} SHUNT CAPACITANCE USED FOR RESONANCE).

(2b) $\sinh \gamma l'_\lambda = \frac{\sinh \gamma l_\lambda}{M}$, V_λ CHOSEN AS IN [2] OR APPROXIMATED BY (6a), (6b).

(2c) $M = \frac{\omega}{\omega_0}$

(2d) $\Delta = \frac{2}{1 + \sqrt{1 - (\lambda_c/\lambda_0)^2}}$

(2e) $\gamma = \frac{2\pi}{\lambda} \sqrt{\left(\frac{\lambda}{\lambda_c}\right)^2 - 1}$

X_0 = CROSS-SECTION DEPENDENT (SEE TEXT)

(2f) $W = \frac{\omega_2 - \omega_1}{\omega_0}$

(2g) $W'_g = 4\phi_0'$

(2h) TABULATED BW $W_g = \left(\frac{W_g''}{W_g'}\right)(2W)$

WHERE $W_g'' = \frac{4\theta_0'}{\pi}$

$\theta_0' = \sin^{-1}\left(\frac{\omega_0}{\omega_1} \sin \pi \frac{\omega_1}{\omega_0}\right) = \sin^{-1}\left(-\frac{\omega_0}{\omega_2} \sin \pi \frac{\omega_2}{\omega_0}\right)$

(3) $\sinh \phi_0' = \frac{\omega_0}{\omega_1} \sinh \left(\omega_0 - \frac{\omega_1}{\omega_0}\right) = -\frac{\omega_2}{\omega_0} \sinh \left(\omega_0 - \frac{\omega_2}{\omega_0}\right)$

(a)

INSERTION LOSS FUNCTION

(4) $\frac{P_0}{P_L} = 1 + h^2 T_N^2 \left[\frac{\omega_0}{\omega} \frac{\sinh \left(\omega_0 - \frac{\omega}{\omega_0}\right)}{\sinh \phi_0'}\right]$

RIPPLE = $10 \log (1 + h^2)$

(5) $h = \frac{V-1}{2\sqrt{V}}$

V = MAXIMUM VSWR

FOR NARROW BAND ONLY

(6a) $V_{0,1} = \frac{2}{\pi} \frac{g_1}{W} = V_{N,N+1}$ WHERE $W = \frac{W_g'}{2}$

(6b) $V_{\lambda,\lambda+1} = \frac{4}{\pi^2} \frac{g_\lambda g_{\lambda+1}}{W^2}$ $\lambda = 1, 2, \ldots (N-1)$

OTHERWISE, USE HALF-WAVE FILTER OR QUARTER-WAVE TRANSFORMER PROTOTYPE TABLES FOR VALUES OF $V_{\lambda,\lambda}$, AS IN [2]. PUBLISHED PROTOTYPE BANDWIDTHS W_g MAY BE USED IF ADJUSTED USING (2h).

PROCEDURE

1) COMPUTE ϕ_0' USING (3).
2) SELECT N USING (4) TO PREDICT STOPBAND RESPONSE.
3) COMPUTE W_g' USING (2g).
4) COMPUTE LENGTHS USING (2a) & (6) OR (2a), (2h) & TABLES.
5) COMPUTE CAPACITORS USING (1a).
6) COMPUTE RESPONSE AND OPTIMIZE

(b)

Fig. 3. Shunt resonators—design formulas.

COMPARISON OF DISTRIBUTED PROTOTYPE RESPONSE TO EVANESCENT RESPONSE

$$\frac{P_0}{P_L} = 1 + h^2 T_N^2 \left[\frac{\omega_0}{\omega} A_i\right]$$

WHERE

$$A_1 = \frac{\sin \pi \frac{\omega}{\omega_0}}{\sin \theta_0'} \quad \text{(DISTRIBUTED)}$$

$$A_2 = \frac{\sinh\left(\omega_0 - \frac{\omega}{\omega_0}\right)}{\sinh \phi_0'} \quad \text{(EVANESCENT, WELL BELOW CUT-OFF)}$$

BW	$\frac{\omega}{\omega_0}$	$\lvert A_1 \rvert$	$\lvert A_2 \rvert$
10%	1.1	2.07	2.03
	1.2	3.95	4.03
	1.3	5.43	6.09
	1.4	6.38	8.22
	1.5	6.71	10.42
20%	1.1	1.1	1.1
	1.2	2.09	2.21
	1.3	2.88	3.35
	1.4	3.39	4.51
	1.5	3.56	5.73
60%	1.3	1.3	1.3
	1.4	1.53	1.76
	1.5	1.6	2.23
	1.6	1.53	2.72
	2.0	0	5.02

(c)

Fig. 3. (*Continued*)

have been rederived for rectangular cross section.

$$\eta_{HE} = \sqrt{\frac{ab}{Dd}} \frac{1 - \left(\frac{D}{a}\right)^2}{\frac{a}{a_g}\cos\frac{\pi D}{2a}} \tag{7}$$

$$B_{HE} = -\frac{1}{\omega\mu}\left\{\frac{a_g}{a}\cot^2\frac{\pi D}{2a} + \frac{a}{D}\eta_H^2 \cdot \left[\frac{b}{a_g}\left\{\left(\frac{\pi}{D}\right)^2 - k^2\right\}\ln\left(\csc\frac{\pi D}{2d}\right) - \frac{a_g}{a}\left(\frac{b}{D}\right)^2\left\{\frac{1}{3} + \frac{1}{2}\left(\frac{d}{b}\right)^2 - \frac{8}{\pi^2}\frac{d}{b}\right\}\right]\right\} \tag{8}$$

where

$$ag = \frac{\lambda_0}{\sqrt{1 - \left(\frac{\lambda_0}{2a}\right)^2}}, \qquad \eta_H = \sqrt{\frac{a}{D}} \frac{1 - \left(\frac{D}{a}\right)^2}{\frac{a}{a_g}\cos\frac{\pi D}{2a}}$$

- a propagating guide width
- b propagating guide height
- D evanescent guide width
- d evanescent guide height

and η_{HE} is the transformation ratio of admittance at the junction. The input sections of such filters are shortened to subtract the discontinuity susceptance computed in (8). Reference planes are shown in Fig. 4.

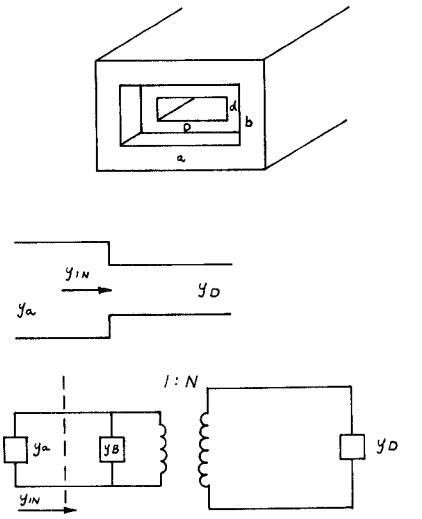

Fig. 4. Waveguide reference plane and definitions of series resonator input step dimensions [1].

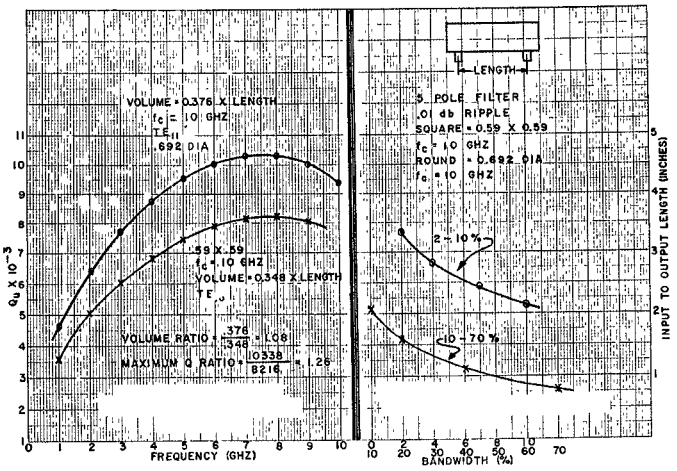

Fig. 5. (a) Q versus frequency (evanescent TE_{10} and TE_{11}). (b) Length versus bandwidth. Round or square cross section.

The design technique can be applied to nonrectangular cross sections. In the Appendix we derive the theoretical unloaded Q for a round cross section excited by an evanescent TE_{11} mode. Plots of round section and square section Qu are shown in Fig. 5 (cutoff frequencies set equal). These Qu data do not include the i^2R_s losses associated with the resonating capacitors. The round-section data should be compared, therefore, to the data in [1]. It is anticipated that inclusion of i^2R_s losses would reduce the Qu somewhat. This work will be accomplished at a later date. Computed filter lengths for identical bandwidths are also shown and are equal. Length is thus dependent solely on the cutoff frequency of the cross section.

Fig. 3 enables computation of the tuning capacitance required for each resonator. It is necessary to subtract the fringing capacity associated with each resonator from the total. At lower frequencies, the resonator may enter the wall of the filter. Fig. 6 illustrates the technique used to compute the total C_t.

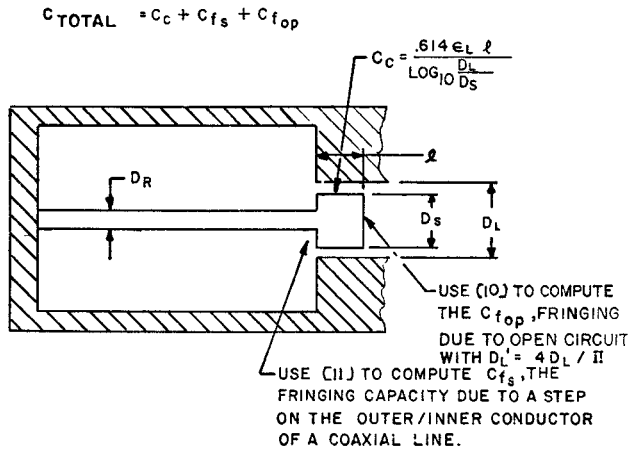

NOTES:
1) IF $\ell \leq D_S$, C_f MUST BE REDUCED AS IN [11] DUE TO PROXIMITY EFFECT.
2) IF RESONATOR CAPACITANCE REQUIRED IS LOW, NO WALL PENETRATION IS NECESSARY. ONLY C_{fop} IS USED (PLUS C_{PP} TO END OF RESONATOR).

Fig. 6. Resonator capacitance realization.

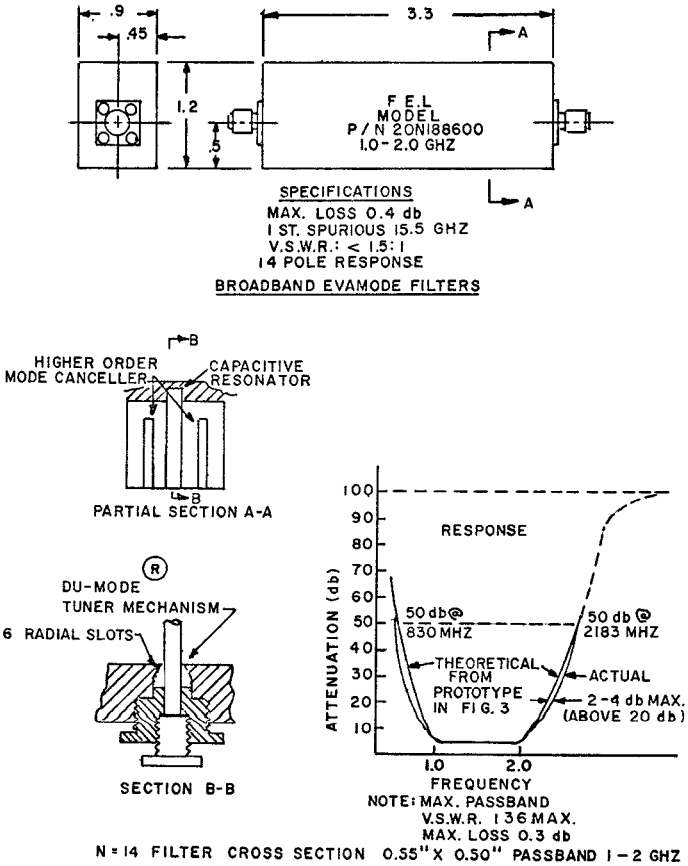

Fig. 7.

To achieve large values of stopband in broad-band filters, it is necessary to suppress the coupling between elements due to the degenerate TE_{20} mode (rectangular cross section). Small-diameter inductive pins are installed (shown in Fig. 7) to perform this function. The effect of the pins is to cancel the coupling between the resonator posts due to the presence of higher order modes [4]. Due to the large end-loading capacity, the pins are capacitive at the resonant frequency of the TE_{10} evanescent mode, but are above series resonance (and thus inductive) at the higher mode frequencies. Using [4], the effect of the pins upon the resonator inductance can be calculated and included into the filter series coupling reactance as previously described. Various methods are available for coupling in and out of the filters. To compute the parameters of the coupling network (9) below, reproduced from [5], can be used.

$$Z_g = -\frac{B}{2A} \pm \sqrt{\frac{1}{4}\left(\frac{B}{A}\right)^2 - \frac{C}{A}} \tag{9}$$

where

$$A = r_{22},\ B = s(X_\Delta + X_{11} r_{22} - X_{22} r_{11})$$
$$C = X_{11} X_\Delta - r_{11} r_\Delta$$
$$\Delta = Z_{11} Z_{22} - Z_{12} Z_{21} = r_\Delta + s X_\Delta.$$

This equation determines the impedance which will conjugately match the input and output of a linear two-port, simultaneously. To use this equation, the impedance matrix of the synthesized filter is constructed, and the resultant elements used in (9). Typically, the coupling element must match into a very low impedance (7 Ω or less) for shunt coupled filters, *a'la'* Fig. 3. Equation (10) approximates the filter input impedance (to be matched) of an evanescent bandpass filter.

$$R_T = \frac{w}{2\pi f_0 C} \tag{10}$$

where

$$w = \frac{f_2 - f_1}{f_0}$$

and C is the required resonating capacitor, determined by Fig. 3.

More exact values for R_T can be obtained by examining the variation in Z_{IN} across the passband, using the matrix cascade as discussed above. Over a 35-percent bandwidth, (10) is accurate enough to achieve input VSWR values of 1.2 maximum. It is necessary to use the matrix cascade computation and the more complex matching method described below, to achieve similarly low VSWR's across greater bandwidth.

Physically, the coupling takes the form of a small loop for bandwidths up to 15 percent and a tap into the first resonator for wider bandwidths. Additionally, for bandwidths greater than 40 percent the coupling may consist of a two- or three-element lumped low-pass filter with different input and output impedances, such that the impedance slope of the coupling more closely matches the impedance versus frequency characteristics of the filter.

For filters starting with series resonators (i.e., waveguide input), the coupling into the first resonator must be modified using (8). For very large cross-section differences between the propagating and cutoff cross section, it is useful to use a capacitive matching screw at the junction to decrease the amount of series inductive discontinuity at the input. With-

out this screw, it is sometimes found that the inductive discontinuity calculated from (8) is so large as to require a negative input length. The use of a foreshortened input section has been discussed, previously, in conjunction with (8). With this screw, a portion of the input inductive discontinuity is "imbedded" into a two-element low-pass filter with cutoff above the desired filter passband. The filter response shown in Fig. 6 results from a filter using shunt input resonators in a cross section measuring 0.5 by 0.5 in. No spurious passbands exist between 2 and 15 GHz. Thus the device stop bandwidth is comparable to that of a combline filter, with a $\lambda/18$ line length. The theoretical unloaded Q can be calculated using [1, (50)]. For the above examples (0.5 by 0.5 in, $f_0 = 1.5$ GHz), $Qu_{\text{theo}} = 3657$.

Through the use of the patented tuner assembly also shown in Fig. 6, we attain about 50 percent of the theoretical excitation value while maintaining the ability to fine tune the center frequency of each element. While [1] referred to recovering 60 percent of the Qu on single sections, actual conversion of the multiple section filter response examples in [1] indicates about 30 percent. Additional tuning screws can be inserted between stubs to effectively decrease or increase (depending upon the plane of insertion) the coupling inductance thus providing "fine tuning." These filters have several mechanisms of spurious response:

1) When the resonator capacitors are spaced $\lambda_g/2$ above cutoff, a passband exists. This occurs from 10 to 100 percent above cutoff, depending upon filter bandwidth (resonator spacing).

2) At twice the TE_{10} cutoff, the second mode (TE_{20} in rectangular) will propagate. The resonators tend to act as short circuits to the TE_{10}, but due to location, will not reduce TE_{20} significantly.

3) The coupling mechanism may resonate.

Filters have been built at 5 GHz with no spurious greater than 80 dB up to 40 GHz. These filters utilized WR-28 cross section (21 GHz f_0). These filters can be folded (with no degradation) for length compensation. Photographs of the inside of such filters are shown (including a folded version of the aforementioned 5-GHz unit. See Fig. 8). Appendix II presents a flow chart showing the method of capacitance calculation.

IV. Applications

1) Bandpass filters with wide stopbands, and extreme package flexibility.

2) Clean-up filters in cascade with cavity filters, yielding low loss and wide stopbands.

3) IF filters. We have used lumped capacitors to realize filters with an unloaded Qu of 400 at 60 MHz in a cross section of 1.5 by 1 in. The filters are loss competitive with helical devices, but are much smaller.

4) In conjunction with item (3) above, the technique can be used to measure the Q of large capacitors (the effective resonating inductance of the cross section is very small). A later paper will present these rather disheartening results (most capacitors are very poor).

5) Component filters in multiplexers.

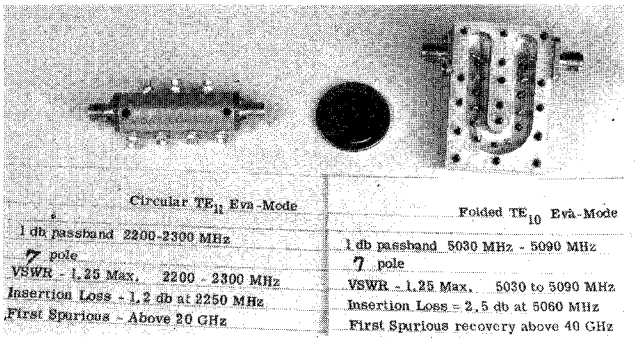

Fig. 8.

V. Comparison to Combline Designs

Fig. 9 presents a comparison of combline filter characteristics with those of the evanescent mode designs. A practical difference is the importance of the inductive stub resonator dimensions in the combline; in the evanescent design, the stub is acting as an extension of one plate of the resonating capacitor. The combline design uses inductive energy storage and fringing capacitance coupling between resonators. The evanescent design uses capacitive energy storage in the local capacitive discontinuities represented by the "stubs," and inductive coupling as shown in Fig. 3. The evanescent design allows arbitrary inversion of the short-circuited end of the resonator; combline designs (to the best of this author's experience) do not.

Equation (27) of [10] presents the Q for slab line interdigital and comb resonators; (50) of [1] and (A8) of this paper present the Q for evanescent rectangular and round designs, respectively. Table I summarizes the results at 1 GHz, comparing a $\lambda/8$ comb design (bar length 1.4765 in) with a 1-in ground plane against an evanescent design with the same internal rectangular cross section (cutoff frequency 3.997 GHz) and against a round evanescent design, diameter = 1.74 in (cutoff = 3.997 GHz). Copper is used in all cases. It can be seen that the spurious performance and unloaded Q of the evanescent designs are superior for the same volume. It is possible that other cross sections (i.e., elliptic) would have even better volume–loss characteristics.

For the same insertion loss and stopband, the evanescent design has been found to be smaller volumetrically than the combline design. The "stub" in an evanescent filter is initially chosen to have very low inductance, i.e., the diameter of the stub is chosen as large as possible within the constraints of TE_{20} coupling or coupling variation due to field changes along the stub, in the filter longitudinal dimension. The nominal stub diameter is about 0.2 times the filter cutoff dimension. In some cases, flat or flattened stubs have been used to minimize stub inductance and the field variation previously described. No noncompensatable response changes occur for diameter variation from 0.1A to 0.25A. Compensation is computed by the iterative inductance apportionment method of Section III, and results in small required changes in the series inductive lengths of waveguide between the capacitive stubs. The inter-

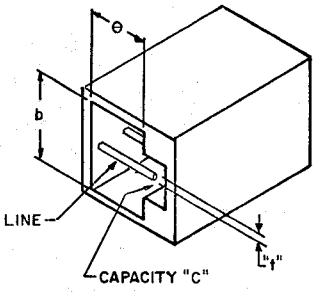

COMB LINE CROSS-SECTION

θ IS FREQUENCY AND SPURIOUS DETERMINING LENGTH
b IS Q-DETERMINING LENGTH

RESONATOR CONSISTS OF THE CAPACITY C RESONATING A SHORT CIRCUITED INDUCTIVE STUB LINE OF THICKNESS t LENGTH θ AND RATIO t/b IN A STRIP LINE OF HEIGHT b. THUS, THE FREQUENCY IS RELATIVELY UNAFFECTED BY CHANGING b, IF t/b IS MAINTAINED. INTER BAR COUPLING IS A STRONG FUNCTION OF t/b.

(a)

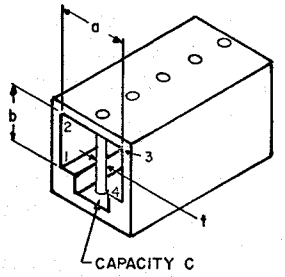

EVA-MODE CROSS-SECTION

a & b CONTRIBUTE TO FREQUENCY AND SPURIOUS DETERMINATION (SEE FIGURE 3)
b IS Q-DETERMINING LENGTH

THE RESONATOR CONSISTS OF THE CAPACITY C RESONATING AN INDUCTANCE FORMED BY THE WALLS OF THE CROSS-SECTION 1, 2, 3, 4. HIGH Q RESULTS FROM THE LARGE VOLUME TO SURFACE RATIO OF THE RESONATED INDUCTANCE. COUPLING IS ALMOST UNAFFECTED BY A CHANGE IN t; EITHER END OF THE "CAPACITY CONDUCTOR" CAN BE SHORT CIRCUITED

(b)

Fig. 9. (a) Combline cross section. (b) Eva-mode cross section.

TABLE I
COMPARISON OF COMB-LINE AND EVA-MODE DESIGNS

Design	Cross Section	Length	Q_u theoretical	Q_u recovered	Spurious
N = 3 comb $\lambda/8$ b = 1" BW = 10%	1.477 x 1.0	3.058 (t/b = 0.4) 3.866 (t/b = 0.2)	3000 (For 75 OHM internal impedance).	2400	4 GHz
N = 3 Rectangular eva-mode BW = 10%	1.477 x 1.0	2.32 ($\frac{d}{a}$ = 0.2)	7500	3575	7.1 GHz
N = 3 round eva-mode BW = 10%	1.74 diameter	2.32	11341	5500	5.3 GHz

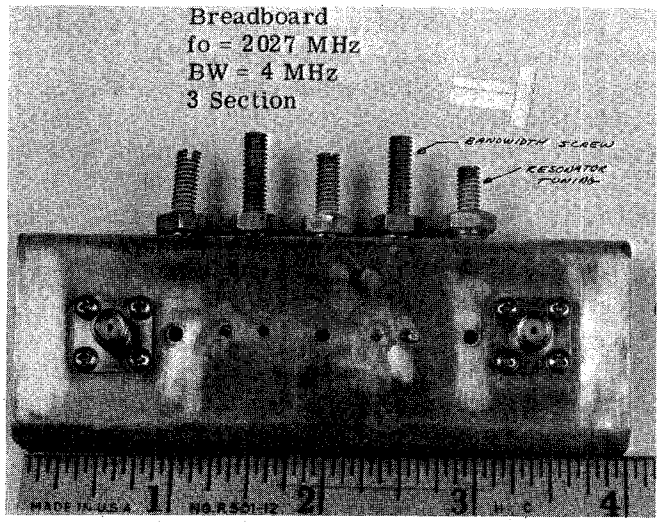

Fig. 10.

connecting lengths of cutoff guide evanescent filter stubs are great enough to effectively suppress (to at least 60 dB) all resonances associated with parallel-bar resonances (used intentionally for combline designs) or to force such resonances to fall into the stopband region of the evanescent structure. To test this theory, a filter was constructed in WR-112 waveguide cross section, but with the "*b*" dimension of Fig. 9(b) being 1.222. The three-element filter had a bandwidth of 4 MHz at a center frequency of 2.0 GHz. For stubs of length 1.122, waveguide width of 0.497, and end capacitance of about 1 pF, quarter-wave resonances would have been expected at about 2.1 GHz. However, no spurious responses greater than −50 dB were observed until 5 GHz, the cutoff of the largest (1.122) dimension. It is possible that the two resonances (evanescent and combline) are in fact one and the same. This should be explored in future work. Additionally, the unit achieved the higher Q predicted from the use of a waveguide with "*b*" greater than "*a*." The physical length of the filter is computed using the cutoff frequency of the 0.497 dimension. The theoretical Q was 5860, with 2300 achieved. A photo is shown in Fig. 10. The crudity of this breadboard certainly contributed to the low recovered Q. However, what is highly significant is that the theoretical Q of a cross section measuring 0.497 square, at 2 GHz, is 4260. We have, therefore, recovered 2300/4260 = 0.54, compared to a 0.497 square section. Standard units, with careful resonator construction, normally recover about 50 percent of the theoretical value. With similar care, we could anticipate a consequent increase in the 2300 value to about 2930. Fig. 11 is an example of a similar series-coupled evamode filter.

VI. Conclusions

We have presented the elements of synthesis and some of the practical considerations necessary for the construction of evanescent filters with bandwidths up to an octave. The filters are lossier than propagating structures, but when it is necessary to cascade a second filter with a propagating filter for spurious suppression, it is often found that the resultant

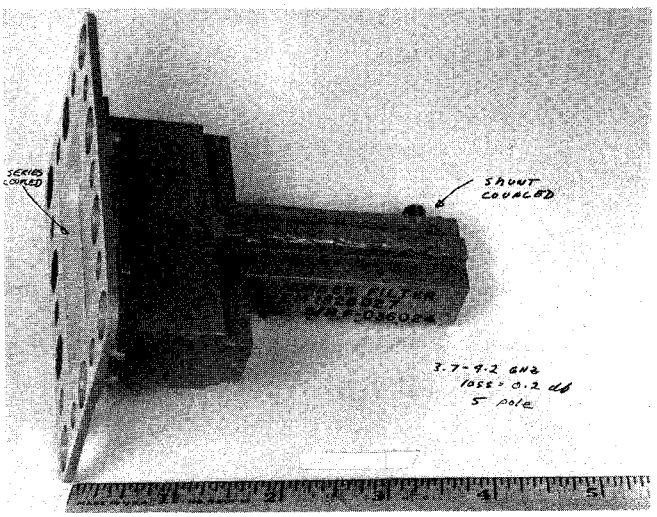

Fig. 11.

net insertion loss is greater than a single evanescent unit. The devices have great packaging flexibility and have about 30 percent less volume than coupled bar designs with equivalent insertion loss; for the same volume, the evanescent design has less loss. The structures are mechanical tolerance-insensitive, and are easy to fabricate. We expect to apply the evanescent high Q lumped tee or pi-equivalent circuit elements to many other networks including tunable filters and equalizers.

Appendix I

Q_U for evanescent TE_{11} (round cross section) filter with

$$H_Z = J_1(k_c r)\cos\Phi$$

$$H_\Phi = j\frac{1}{\eta}\left(1-\frac{f_c^2}{f^2}\right)^{1/2}\frac{\eta}{k_c r}\frac{f}{f_c}J_1(k_c r)\sin\Phi$$

$$H_r = -j\frac{1}{\eta}\left(1-\frac{f_c^2}{f^2}\right)^{1/2}\eta\frac{f}{f_c}J_1'(k_c r)\cos\Phi$$

$$E_r = j\frac{\eta}{k_c r}\frac{f}{f_c}J_1(k_c r)\sin\Phi$$

$$E_\Phi = j\eta\frac{f}{f_c}J_1'(k_c r)\cos\Phi$$

$$\eta = \sqrt{\frac{\mu}{\varepsilon}}. \tag{A1}$$

Maximum stored energy

$$W = \frac{\mu}{2}\iiint_v H\cdot H^*\,dV. \tag{A2}$$

Average dissipated power

$$P = \frac{R_s}{2}\iint_{\text{walls}} H_{\tan}\cdot H_{\tan}^*\,ds. \tag{A3}$$

Substitute (A1) into (A2)

$$W = \frac{\mu}{2}\int_v (H_Z^2 + H_\Phi^2 + H_r^2)\,dv.$$

After algebra

$$W = \frac{\pi\mu}{2}\int_0^L e^{-2rz}\,dz\left[\int_0^a J_1^2(k_c r)r\,dr + \int_0^a \frac{1}{k_c^2}\left(1-\frac{f^2}{f_c^2}\right)\frac{1}{r}J_1^2(k_c r)\,dr + \int_0^a\left(1-\frac{f^2}{f_c^2}\right)J_1'^2(k_c r)r\,dr\right]. \tag{A4}$$

Substitute (A1) into (A3)

$$P = \frac{R_s}{2}\int_0^{2\pi}\int_0^L |H_Z|^2_{r=a}\,a\,d\Phi\,dz + \int_0^{2\pi}\int_0^L |H_\Phi|^2_{r=a}\,a\,d\Phi\,dz. \tag{A5}$$

After algebra

$$P = \frac{\pi a R_s}{2}\int_0^L e^{-2rz}\,dz J_1^2(k_c a)\left[1+\frac{(1-f^2/f_c^2)}{k_c^2 a^2}\right]. \tag{A6}$$

Dividing (A4) by (A6), and letting $k_c r = v$ result in

$$Q_U = \frac{\omega\mu a}{R_s}\frac{A + (1-f^2/f_c^2)[B+C]}{J_1^2(k_c a)[k_c^2 a^2 + (1-f^2/f_c^2)]} \tag{A7}$$

where

$$A = \left(\frac{k_c a}{m}\right)^2\sum_{\eta=1}^{m}(m-\tfrac{1}{2})J_1^2\left[\frac{k_c a}{m}(m-\tfrac{1}{2})\right] \cong \int_0^{k_c a} v J_1^2(v)\,du$$

$$B = \sum_{\eta=1}^{m}\frac{J_1^2[k_c a/m(m-\frac{1}{2})]}{m-\frac{1}{2}} \cong \int_0^{k_c a} J_1^2(v)\frac{dv}{v}$$

$$C = \frac{1}{4}\left(\frac{k_c a}{m}\right)^2\sum_{\eta=1}^{m}(m-\tfrac{1}{2}) \cdot \left[J_0\left(\frac{k_c a}{m}(m-\tfrac{1}{2})\right) - J_2\left(\frac{k_c a}{m}(m-\tfrac{1}{2})\right)\right]^2 \cong \int_0^{k_c a} v J_1'^2(v)\,dr.$$

For TE_{11} mode, $k_c a = 1.84$ after evaluation of terms

$$Q_U = \frac{\pi f\mu d}{R_s}\left[\frac{0.404 + 0.405(1-f^2/f_c^2)}{1.144 + 0.338(1-f^2/f_c^2)}\right] \tag{A8}$$

where d is the diameter of cross section and f_c is the cutoff frequency for cross section.

APPENDIX II
FLOW CHART FOR RESONATOR END CAPACITANCE CALCULATION

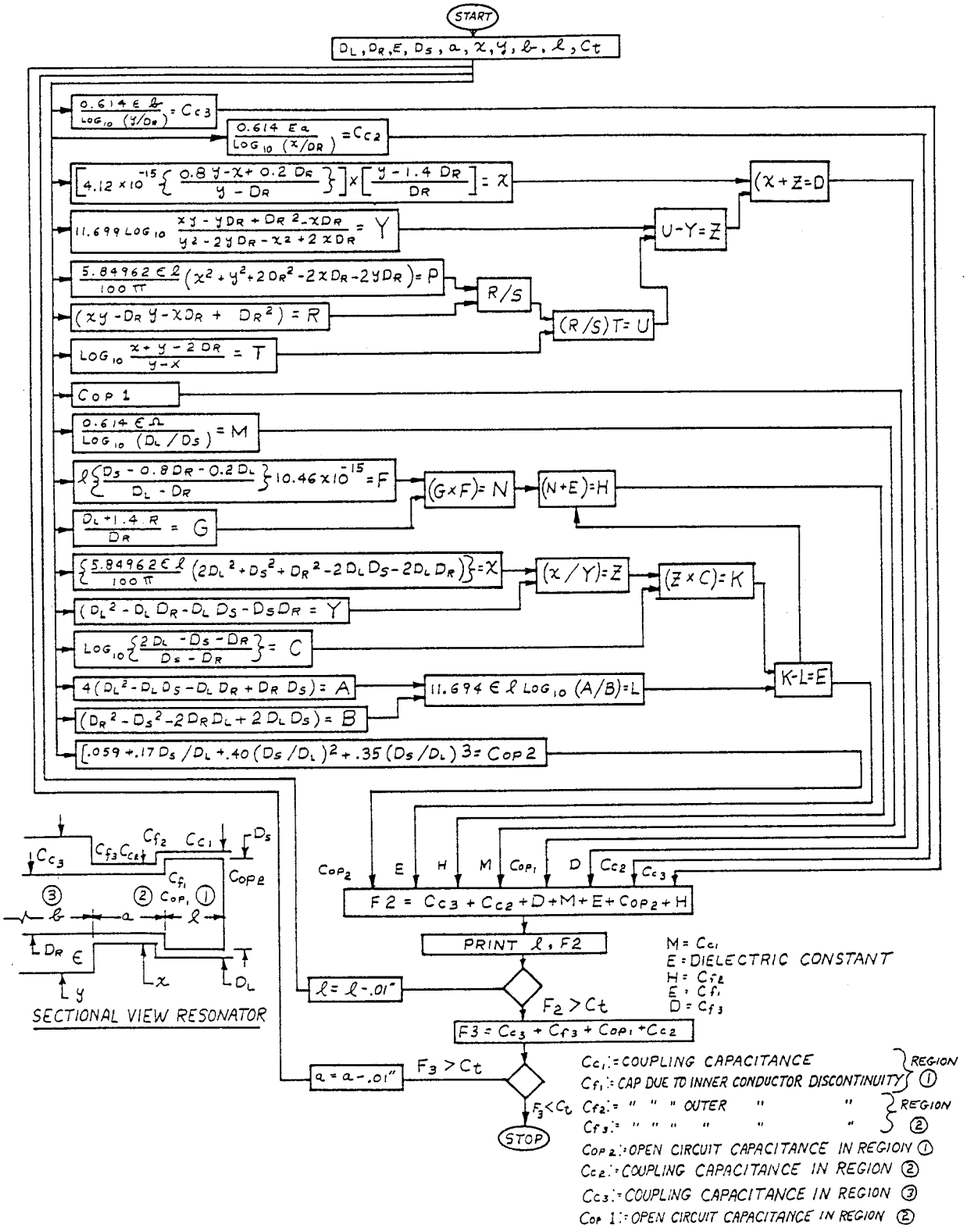

REFERENCES

[1] G. F Craven and C. K. Mok, "The design of evanescent mode waveguide bandpass filters for a prescribed insertion loss characteristic," *IEEE Trans. Microwave Theory Tech.*, vol. MTT-19, pp. 295–308, Mar. 1971.

[2] R. Levy, "Theory of direct-coupled cavity filters," *IEEE Trans. Microwave Theory Tech.*, vol. MTT-15, June 1967.

[3] L. Lewin, *Advanced Theory of Waveguides*. New York: Illife, 1951, pp. 88–100.

[4] ——, *Theory of Waveguides*. Halsted Press, 1975, sec. 5.13.

[5] R. Snyder and D. Bozarth, "Source and load impedance for simultaneous conjugate match of linear 2 port," *Electronic Communicator*, Nov./Dec. 1967.

[6] G. F. Craven and L. Lewin, "Design of microwave filters with quarter wave couplings," *Proc. Inst. Elec. Eng.*, Part B, vol. 103, no. 8, pp. 173–177, Mar. 1956.

[7] R. Ghose, *Microwave Circuit Theory and Analysis*. New York: McGraw-Hill, 1963, pp. 168–171.

[8] C. K. Mok, "Design of evanescent-mode waveguide diplexers," *IEEE Trans. Microwave Theory Tech.*, vol. MTT-21, pp. 43–48, Jan. 1973.

[9] W. Edson, "Microwave filters using ghost-mode resonance," presented at Electronic Components Conference, San Francisco, May 2–4, 1961.

[10] B. F. Nicholson, "Practical design of interdigital and combline filters," *Radio and Electronic Engineer*, pp. 44–45, July 1967.

[11] P. Somlo, "Computation of coaxial line step capacitances," *IEEE Trans. Microwave Theory Tech.*, vol. MTT-15, Jan. 1967.

Dual-Mode Canonical Waveguide Filters

ALBERT E. WILLIAMS, MEMBER, IEEE, AND ALI E. ATIA, MEMBER, IEEE

Abstract—**This paper introduces a new form of dual-mode narrow-bandpass waveguide cavity filter. The filters, which can be constructed from either dual mode circular or square waveguide cavities, can realize the optimum transfer functions (including the exact elliptic function response). One of the unique features of these filters is that all the intercavity coupling irises may take the form of circular holes rather than long narrow slots. Several alternative input–output configurations are described. Experimental results on several filters indicate excellent agreement with theory.**

INTRODUCTION

THE DEVELOPMENT of high-capacity communications satellite transponders has made it necessary to channelize the frequency spectrum to efficiently use the available spacecraft transmit power. To accomplish this objective, filter guard bands must be minimized and hence sharp frequency selectivity is required. Further, the filters must have flat in-band gain slope and small group-delay variation to minimize communications cross talk and distortion. Therefore, the need for high-performance microwave channelizing filters which possess optimum responses consistent with minimum weight and volume is apparent.

Starting with the cascaded waveguide cavity (Chebyshev or Butterworth design [1]), the development of the linear phase filter [2], the dual-mode (TE_{111}) longitudinal circular cavity filter [3], and the single-mode rectangular (TE_{101}) and dual-mode square (TE_{101}) folded geometries [4] are evidence of the improvement which has occurred in recent years. The key to the developments is the recognition that simple cascaded waveguide cavity filters cannot have finite transmission zeros. On the other hand, the optimum filter must have the maximum possible number of finite transmission zeros, placed at predetermined (arbitrary) locations in the complex frequency plane, as may be dictated by the solution of the approximation problem.

A possible configuration for obtaining the most general response from a set of n-multiple-coupled synchronously tuned cavities is the canonical form [5]. In this form, the cavities are numbered 1 to n, with the input and output ports located in cavities 1 and n, respectively. Cascade (or series) couplings of the same sign must be provided between consecutively numbered cavities, i.e., 1 to 2, 2 to 3, $\cdots, n-1$ to n (as in the Chebyshev filter). In addition, shunt (or cross) couplings of arbitrary signs must be provided between cavities 1 and n, 2 and $n-1$, $\cdots$, etc. As in the canonical form, the more general responses which can be obtained from multiple couplings allow a given filter specification to be met by fewer electrical cavities, which in turn leads to minimum weight and volume.

The canonical coupling set may be realized with the single-mode or dual-mode folded geometries, but its realization in the simpler longitudinal dual-mode circular (or square) cavity geometry has not been described. Therefore, the advantages of the longitudinal dual-mode filter, such as minimum weight and volume and ease of fabrication, do not coincide with the optimum filter response.

This paper presents a new dual TE_{111} mode circular waveguide cavity structure, the dual mode canonical filter, which realizes the optimum electrical response, and retains all the mechanical advantages of the longitudinal dual-mode filter. This filter is described with reference to its equivalent circuit. Its design is outlined, with specific emphasis on the design of its input and output ports. Detailed experimental results for four-pole elliptic filters indicate the validity of the design philosophy. Finally, experimental results for six- and

Manuscript received May 11, 1977; revised August 8, 1977. This paper was supported by the International Telecommunications Satellite Organization (INTELSAT).

The authors are with COMSAT Laboratories, Clarksburg, MD 20734.